



Hydrothermally Derived $\text{Cu}_2\text{ZnSnS}_4$ Nanocomposite for Photovoltaic Applications

Jitendra P. Sawant¹ & Rohidas B. Kale^{1*}

¹ Department of Physics, The Institute of Science, Madam Cama Road, Mumbai-400032, INDIA

* Correspondence: E-mail: rb_kale@yahoo.co.in

(Published 03 Mar, 2018)

ABSTRACT: $\text{Cu}_2\text{ZnSnS}_4$ nanocomposites were synthesized via facile hydrothermal method. The structural, compositional and morphological properties were investigated. The X-ray diffraction study revealed that the $\text{Cu}_2\text{ZnSnS}_4$ synthesized exhibit, kesterite phase $\text{Cu}_2\text{ZnSnS}_4$. The field emission scanning electron microscope images showed the highly compact microsphere morphology. Copper-rich and zinc-poor composition were detected by the Energy dispersive spectroscopic analysis, which is suitable for best photovoltaic effect. UV-visible spectroscopy analysis showed strong absorption in visible range. The direct band gap of $\text{Cu}_2\text{ZnSnS}_4$ nanocomposite was estimated to be of 1.56 eV.

Keywords: CZTS nanocomposite; Hydrothermal growth; Kesterite Phase; Morphological properties; Optical Properties and Photovoltaics.

INTRODUCTION: Properties shown by nanoscale materials are different from those of their bulk materials. For this reason, synthesis and optimization technique for production of nanoparticles have been intensively investigated during the last few decades. In solar cell device light absorber material plays a key role. It has optimum direct band gap around 1.5 eV, earth-abundant composition, and high absorption coefficient $> 10^4 \text{ cm}^{-1}$ [1-3]. The CZTS compound exist in kesterite and stannite phase with space group $\Gamma 4$ and $\Gamma 42m$ respectively [4, 5]. These phases belong to tetragonal structures, with cubic closely packed array of sulfur as an anions, and cations positioning at one half of the tetrahedral voids, with a stacking similar to zincblende with lattice constant $a = 5.46 \text{ \AA}$ and $c = 10.93 \text{ \AA}$ [6]. The $\text{Cu}_2\text{ZnSnS}_4$ (CZTS) nanocomposite is challenging light absorber material, has drawn world-wide attention due to its outstanding performance in photovoltaic applications. Nanocrystalline CZTS have potential applications as counter electrodes for high efficiency dye-sensitized solar cells [7-9].

CZTS nanocrystalline materials have been synthesized using hot-injection method [10]. Hierarchical CZTS particle were synthesized using solvothermal process [11, 12]. However, an environment-friendly and low-cost route for synthesis of high quality CZTS, such as hydrothermal method is highly desirable. Hydrothermal synthesis does not require any expensive precursors or equipment. In the current work, CZTS nanocomposite was synthesized using hydrothermal route and water as a solvent. The structural, optical and

morphological properties of CZTS nanocomposite were studied by varying the molar concentration of precursor solution.

MATERIAL AND METHODS: All AR grade chemicals were purchased from S. D. Fine Chem. Ltd. and used without further purification. Initially an appropriate amount of (0.01M) CuSO_4 , (0.01M) ZnSO_4 , (0.01M) SnCl_2 and (0.04M) $\text{SC}(\text{NH}_2)_2$ dissolved in 250 ml of doubled distilled water. The resultant solution was stirred for 10 to 15 minutes and transferred in to Teflon-lined stainless-steel autoclave filled up to 75% of its capacity. The autoclave was kept in hot air oven maintained at temperature of 180°C or 24 h, without stirring during heating. After completion of reaction time, autoclave was allowed to cool naturally at room temperature. The final product was dried in air at 80°C for 4-6 h and used for further characterizations. The experiment was repeated with 0.03M and 0.05M metal ion precursors while 0.12M and 0.2M sulfur precursor. The samples prepared were named as A1, A2 and A3 respectively.

For phase identification, X-ray diffraction (XRD) patterns were recorded using XPERT-PROMPD X-ray diffractometer, with CuK_α radiation ($\lambda = 1.5405 \text{ \AA}$) in 2θ range of $20-80^\circ$. The surface morphology and composition of samples were studied by scanning electron microscopy (FESEM) (JEOL, JSM-IT300) equipped with energy dispersive X-ray spectroscopy (EDS). The optical properties of the material were studied by UV-Vis (Shimadzu UV 1800) absorbance spectrophotometer in wavelength range 400 to 1100

nm at room temperature. The absorbance spectrum was measured by ultrasonically dispersing the powder sample in ethanol.

RESULTS AND DISCUSSION:

Phase analysis by XRD: Figure 1 shows the XRD pattern of CZTS nanocomposite. For all the three samples (A1, A2, A3) of different solution concentration, major diffraction peaks seen at $2\theta = 28.5^\circ, 47.6^\circ$ and 56.6° , which are assigned to the (112), (220) and (312) planes (JCPDS 26-0575). According to Scherrer's equation, the grain size is estimated to be about 5 nm from the (112) diffraction peak. Formation of CZTS is initiated by the formation of Cu_{2-x}S nanocrystals as a result of reduction of Cu²⁺ to Cu⁺. This is followed by the rapid diffusion of cations Sn⁴⁺ and Zn²⁺ to the crystal framework of Cu_{2-x}S to form CZTS [13]. It can be seen from figure that at lower precursor concentration (A1) secondary phases like CuS, Cu₂ZnSn₃ were observed. This may be because of non-decomposition of binary phases during formation of CZTS compound. However, at higher precursor concentration (A3), these phases were decomposed into CZTS nanocomposit.

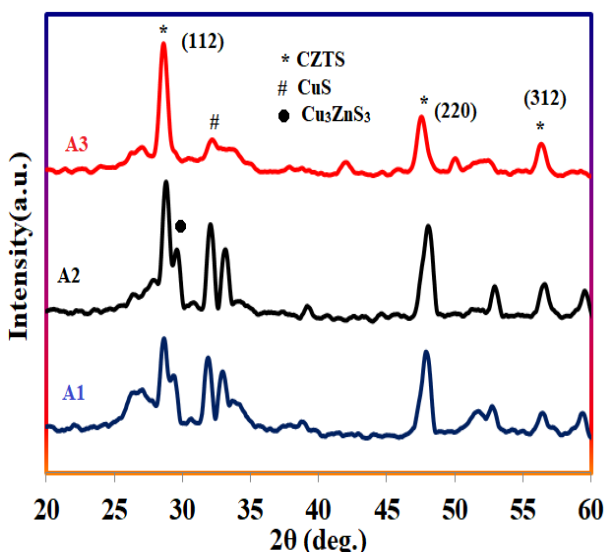


Figure 1: XRD pattern of the CZTS nanocomposite synthesized with different molar concentration.

Morphological and compositional analysis: Figure 2 (A1-A3) represents the FESEM images of CZTS nanocomposite. Inset of the figure 2 (A2) shows the distribution of microsphere of diameter with 1 to 3µm. The microspheres are covered with spherical grains typical size around 100 nm in diameter. At higher concentration the chain of interconnected spherical grains formed. Closer inspection of figure 2(A3) revealed that the microspheres become more compact with interconnected spherical grain. In order to under-

stand the composition of CZTS nanocomposite EDS analysis was carried out. Figure 3 represents elemental composition of CZTS nanocomposite with variation of precursor concentration. It is clear that the sample prepared was near stiochiometric.

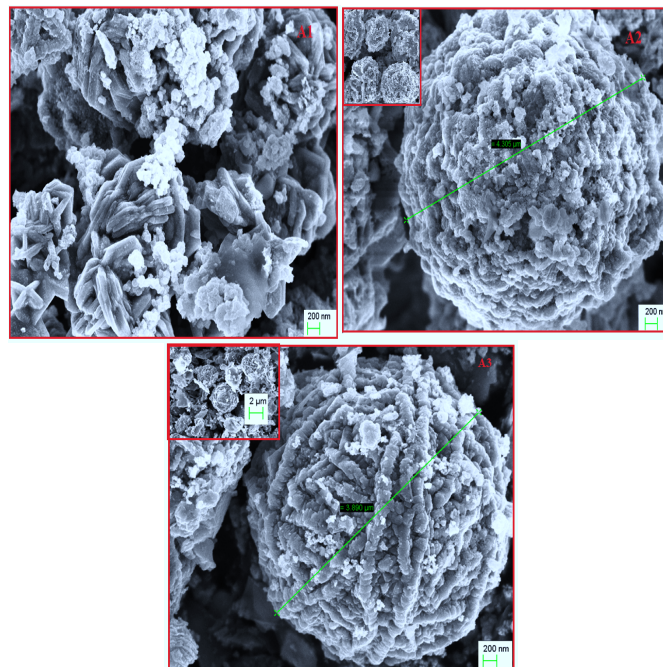


Figure 2: FESEM images CZTS nanocomposite of three different compositions.

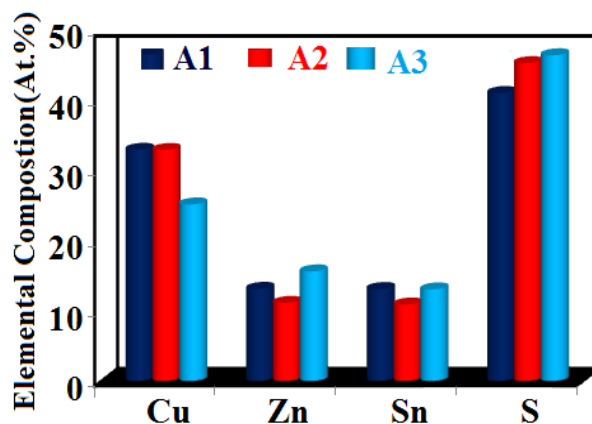


Figure 3: Histogram showing the comparison of elemental composition in CZTS nanocomposite.

Table1: Elemental composition of CZTS nanocomposite.

Sample	Cu	Zn	Sn	S
A1 Cu, Zn, Sn-0.01 M and S-0.04	32.87	13.10	13.08	40.94
A2 Cu, Zn, Sn-0.03M and S-0.12 M	32.84	11.10	10.87	45.19
A3 Cu, Zn, Sn-0.05 M and S-0.4M	25.10	9.58	19.02	46.30

Optical study: The band gap was estimated by plotting the graph of $(\alpha h\nu)^2$ vs $(h\nu)$ and extrapolating with energy axis as shown in figure 4. The value of band gap for CZTS nocomposite was estimated to be 1.56 eV. The band gap was found to be strongly dependent on the particle sizes of the products [15]. The structure may also affect the band gap of the product.

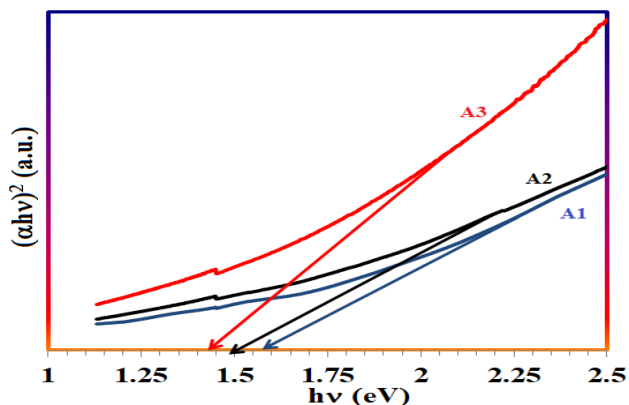


Figure 4: $(\alpha h\nu)^2$ vs $(h\nu)$ plot of CZTS nanocomposite synthesized using three different solution compositions.

CONCLUSION: CZTS naocomposite were successfully synthesized using low cost, environment friendly hydrothermal method. It is investigated that the change of precursor concentration of solution affects the structural and morphological properties of CZTS nanocomposits. All the sample showed kesterite phase CZTS. However, at lower precursor concentration, CuS and Cu₃ZnSnS₃ phases were observed. The FESEM images of CZTS product reveled compact microsphere with 2 to 5 μm diameter. EDS data reveled that, Cu rich and Zn poor product. From UV-Vis absorption analysis direct band gap of 1.56 eV for microspheres were estimated.

ACKNOWLEDGEMENT: This research work is supported by the Department of Science and Technology, India under DST-FIST (SR/FST/PSI-173/2012) program. Authors are thankful to Director, The Institute of Science, Mumbai, for encouragement and providing the necessary facilities. Authors are also thankful to INUP, as a part of the reported work (characterization) was carried out at the IITBNF, IITB under INUP which is sponsored by DeitY, MCIT, Government of India.

REFERENCES:

1. Ramasamy, K., Malik, M. A., O'Brien, P. (2012) Routes to copper zinc tin sulfide Cu₂ZnSnS₄ a potential material for solar cells, *Chemical Communications*, 48(46), 5703–5714.
2. Fairbrother, A., García-Hemme, E., Izquierdo-

3. Roca, V., Fontané, X., Pulgarín Agudelo, F. A., Vigil-Galán, O., Pérez-Rodríguez, A., Saucedo, E. (2012) Development of a selective chemical etch to improve the conversion efficiency of Zn-rich Cu₂ZnSnS₄ solar cells, *Journal of American Chemical Society*, 134(19), 8018–8021.
4. Chen, S. Y., Walsh, A., Gong, X. G., Wei, S. H. (2013) Classification of lattice defects in the kesterite Cu₂ZnSnS₄ and Cu₂ZnSnSe₄ earth-abundant solar cell absorbers, *Advanced Materials*, 25(11), 1522–1539.
5. Hall, S. R., Szymanski, J. T., Stewart, J. M. (1978) Kesterite, Cu₂(Zn,Fe)SnS₄, and stannite, Cu₂(Fe,Zn)SnS₄, structurally similar but distinct minerals, *The Canadian Mineralogist*, 16(2), 131–137.
6. Paier, J., Asahi, R., Nagoya, A., Kresse, G. (2009) Cu₂ZnSnS₄ as a potential photovoltaic material: A hybrid Hartree-Fock density functional theory study, *Physical Review B*, 79(11), 115126 (1-8).
7. Guo, Q. J., Hillhouse, H. W., Agrawal, R. (2009) Synthesis of Cu₂ZnSnS₄ nanocrystal ink and its use for solar cells, *Journal of American Chemical Society*, 131(33), 11672–11673.
8. Xin, X. K., He, M., Han, W., Jung, J. H., Lin, Z. Q. (2011) *Angew Chem Int Ed* 50(49)11739–11742.
9. X, u, J., Yang, X., Yang, Q. D., Wong, T. L. (2012) Cu₂ZnSnS₄ Hierarchical Microspheres as an Effective Counter Electrode Material for Quantum Dot Sensitized Solar Cells, *Journal of Physical Chemistry C*, 116(37), 19718–19723.
10. Dai, P. C., Zhang, G., Chen, Y. C., Jiang, H. C., Feng, Z. Y., Lin, Z., Zhan, J. H. (2012) Porous copper zinc tin sulfide thin film as photocathode for double junction photoelectrochemical solar cells, *Chemical communication*, 48(24), 3006–3008.
11. Riha, S. C., Parkinson, B. A., Prieto, A. L., (2009) Solution-based synthesis and characterization of Cu₂ZnSnS₄ nanocrystals, *Journal of American Chemical Society*, 131(34), 12054–12055.
12. Zhou, Y. L., Zhou, W. H., Du, Y. F., Li, M., Wu, S. X. (2011) Sphere-like kesterite Cu₂ZnSnS₄ nanoparticles synthesized by a facile solvothermal method, *Material Letters*, 65(11), 1535–1537.
13. Chen, L. J., Chuang, Y. J. (2013) Quaternary semiconductor derived and formation mechanism by non-vacuum route from solvothermal nanostructures for high-performance application, *Material Letters*, 91, 372–375.
14. Vincent, T. T., John, B., Wang, H. (2014) One-

step synthesis of high quality kesterite Cu₂ZnSnS₄ nanocrystals – a hydrothermal approach, *Beilstein Journal of nanotechnology*, 5, 438–446.

14. Sarkar, S., Bhattacharjee, K., Das, G. C., Chattopadhyay, K. K. (2014) Self-sacrificial template directed hydrothermal route to kesterite-Cu₂ZnSnS₄ microspheres and study of their photo response properties, *Cryst Eng Comm*, 16, 2634.
15. Xie, R. G., Rutherford, M., Peng, X. G. (2009) Formation of high-quality I-III-VI semiconductor nanocrystals by tuning relative reactivity of cationic precursors, *Journal of American Chemical Society*, 131, 5691–5697.